applied sciences

MDPI

Article

Analytical and Numerical Study on the Stability of Highway Subgrade with Embedded Loading Berm in Soft Soil Area

Feng Xiong *, Xuebin Wang, Fan Yang, Jiaqiang Yang, Li Hu and Rui Li

School of Civil Engineering, Hefei University of Technology, Hefei 230051, China
* Correspondence: cvexf@hfut.edu.cn

Abstract: Loading berm is an effective method for improving highway subgrade stability in soft soil areas. However, this method requires lots of construction space. It is not applicable in some areas with narrow construction spaces. To address this problem, an embedded loading berm (ELB) is proposed to improve highway subgrade stability, and the effects of ELB on the stability of the highway subgrade were investigated by analytical and numerical methods. Firstly, an analytical model was proposed to analyze the relationship between the ELB dimensions and subgrade stability factors. Then, numerical simulations were carried out to further reveal the stability factor of an actual subgrade with different ELBs. Lastly, ELB parameters' sensitivity to the ELB stability factors was studied. The results show that the stability of the highway subgrade in soft soil areas can be significantly improved by the proposed ELB. With the loading berm width and height increasing, the subgrade stability factors can increase. The stability factors' increase ratio with the increased ELB width is greater than that with the increased ELB height. The ELB parameter sensitivity order on the subgrade stability is as follows: width > height > density > cohesion > internal friction. In the design process, the ELB width and height can be mainly focused on. The research is significant for promoting the application of ELB in soft soil areas.

Keywords: highway subgrade; embedded loading berm; stability factor; parameter sensitivity

Citation: Xiong, F.; Wang, X.; Yang, F.; Yang, J.; Hu, L.; Li, R. Analytical and Numerical Study on the Stability of Highway Subgrade with Embedded Loading Berm in Soft Soil Area. *Appl. Sci.* **2022**, *12*, 12440. https://doi.org/10.3390/app122312440

Academic Editor: Raffaele Zinno

Received: 19 October 2022
Accepted: 1 December 2022
Published: 5 December 2022

1. Introduction

In the Chinese coastal areas, the economy is developed and more and more highways need to be built. However, in these areas, there are large areas of soft soil which has the characteristics of large porosity ratio, high water content, high compressibility, and low strength. When the highways are constructed on soft soil, the subgrade's large settlement or uneven settlement will occur [1,2]. This is very harmful to subgrade stability. Therefore, the soft soil base should be treated to improve the highway subgrade stability.

The loading berm is a treating measure of the soft soil base. The implementation method is as follows. As shown in Figure 1, on both sides of the subgrade, the compacted soil is put on the soft soil base and then the loading berm is formed. The loading berm can inhibit the lateral uplift trend of the soft soil and improve the subgrade stability. Its effectiveness is larger than that of a cutting slope [3]. Due to the good performance of the loading berm, it is widely used for highways in soft soil areas.

However, there are also some new cases in the loading berm application. For example, due to the large area of the loading berm, there is not enough construction space in some sections [4]. So, the loading berm cannot be used in these sections. To address this problem, an embedded loading berm (ELB) is proposed in this paper. As shown in Figure 2, the compacted soil is embedded into the soft soil to form the ELB. Compared to the loading berm, the ELB width is smaller. The ELB height can be increased to meet the subgrade stability requirement. The ELB can also inhibit the lateral uplift trend of the soft soil and improve the subgrade stability. Furthermore, the ELB can save construction space and reduce the disturbance effect on the surrounding environment.

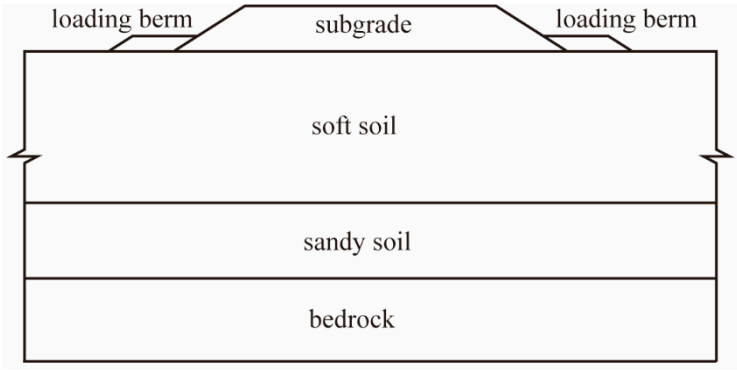

Figure 1. Schematic diagram of loading berm.

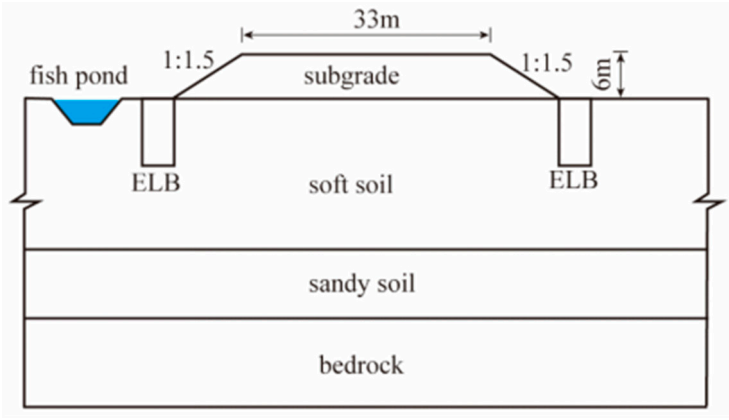

Figure 2. Profile of subgrade reinforced by ELB.

To date, lots of research has been carried out on the failure modes and stability factors of subgrade in soft soil areas. These studies mainly focused on the influences of loading berm height and width on the subgrade stability factors. Zhang et al. [4] established a stability calculation model of the highway subgrade base on the Mombasa–Nairobi Standard Gauge Railway. They concluded that the loading berm is more advantageous than the gravel pile during the construction period. Corkum et al. [5] found that the landslide displacement can be effectively controlled by setting a small loading berm at the slope foot. Through physical modeling and field monitoring, Zaytsev et al. [6] found that subgrade settlement can be effectively diminished by increasing the height of the loading berm. Viswanadham et al. [7] studied the stability of the railway subgrade constructed by fly ash. The study shows that when the subgrade height is 11 m, the loading berm height should not be less than 1.5 m. Chen and Song [8] proposed the optimization design method of a single-step loading berm and the simplified calculation method of stability factor. They also verified the applicability of the method. Zhao et al. [9] deduced the slipping surfaces equilibrium equation considering the cohesion and internal friction angle. Based on the equilibrium equation, a method was presented for determining the reasonable width and height of the loading berm. ISAMU [10] brought out a method to determine the dimensions of loading berm using arc law.

Recently, lots of studies were conducted on the subgrade slope stability by the numerical calculation method [11–16]. In 1975, Zienkiewicz et al. [17] first applied the strength reduction method to slope stability analysis. Ma et al. [18] researched the stability of a typical three-dimensional slope by the local strength reduction method (LSRM) and explored the feasibility of the local strength reduction method. The results show the local strength reduction method is feasible. Using the strength reduction method, Zhang et al. [19] analyzed the stability of the subgrade with loading berm under different working conditions. The stability was compared with those calculated by the limit equilibrium method. The

results show the stability calculated through the strength reduction method was closer to the actual engineering situation [20–22].

To sum up, many scholars have carried out lots of studies on the subgrade with loading berm in soft soil areas. However, there are few studies on the stability of the highway subgrade with the ELB.

In this study, the stability of highway subgrade with the ELB was researched using analytical and numerical simulation methods. Firstly, an analytical model was proposed to describe the relationship between the ELB dimensions and the subgrade stability factors. Then, numerical simulations were carried out to reveal the stability factor of an actual subgrade with different ELB widths and heights. Lastly, the sensitivity of ELB parameters to the ELB stability factors is discussed. The research provides references for ELB design and is significant for promoting the application of ELB in soft soil areas.

2. Engineering Background

Marine soft soil is distributed widely in the Yancheng area of Jiangsu Province, China. The Yancheng-Lianyungang Highway crosses an island that is rich in water. The strata of the island are mainly divided into three layers. The upper layer includes a variety of soft soils. The middle layer is sandy soil. The lower layer is the bedrock, as shown in Figure 2. The width of the subgrade top is 33 m, and the subgrade height is 6 m. The slope angle of the subgrade is 1:1.5. To keep the subgrade stable, the loading berm was used in this engineering. However, on the north side of the island, there is a large-scale fish pond near the subgrade. The fish pond cannot be expropriated. Near the fish pond, there are not enough constructed spaces for the loading berm. In this paper, an embedded loading berm (ELB) is proposed to address the problem. The ELB means that the berm is embedded into the soft soil. The ELB width is smaller than that of the loading berm and then the construction space is saved. To meet the subgrade stability requirement, the ELB height should be increased. The materials of the ELB can be the same as those of the subgrade. The ELB can save construction space to protect the fish pond. However, the influence of ELB on subgrade stability is unclear.

3. Analytical Model for the Highway Subgrade Stability

3.1. The Relationship between the Subgrade Stability Factors and the ELB Width

The ELB and subgrade were made from compacted soil. Their strength is much greater than that of the soft soil. When the ELB strength is not enough, the subgrade is prone to shear failure as shown in Figure 3. To quantitatively analyze the subgrade stability factor, the following assumptions are made. The position of the sliding surface does not change with the increase in subgrade width and height. That is, h_1 remains unchanged.

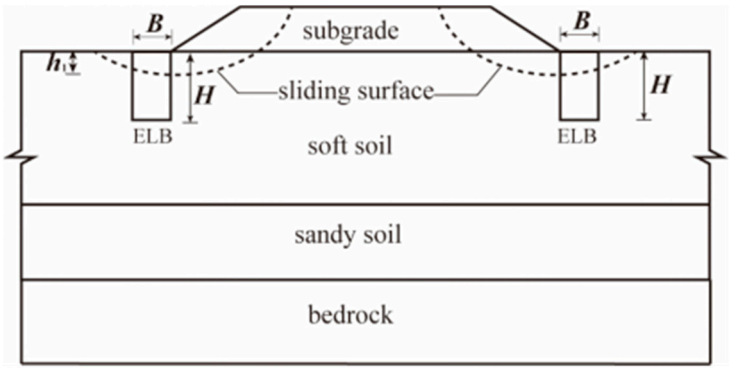

Figure 3. Diagram of the subgrade shear failure mode.

When the ELB cannot provide adequate resistance, subgrade shear failure will occur and the ELB breaks along the sliding surface. The ELB can be divided into two parts by the sliding surface, as shown in Figure 4. Part I is above the sliding surface while part II

is below the sliding surface. The force on part I is demonstrated in Figure 4. The passive earth pressure on part I is E_p. The landslide pushing force on part I from the sliding body is F_n. The force on part I from part II is f. When part I is in a critical state, then

$$F_n = E_p + f \tag{1}$$

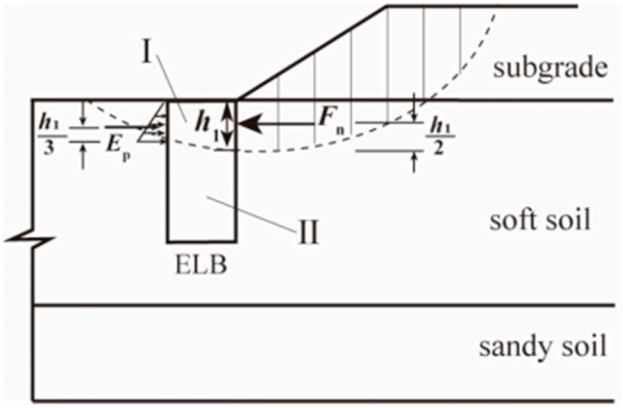

Figure 4. Shear failure diagram of the ELB.

The landslide body can be divided into many separate blocks. The landslide pushing force F_n can be calculated by the limiting equilibrium theory and the transfer coefficient method. The detailed calculation process is performed using the following equation.

$$F_n = F_{n-1}\psi_n + F_s G_n \sin\beta_n - G_n \cos\beta_n \tan\varphi_n - c_n l_n \tag{2}$$

$$\psi_n = \cos(\beta_{n-1} - \beta_n) - \sin(\beta_{n-1} - \beta_n)\tan\varphi_n \tag{3}$$

where F_n, F_{n-1} are the residual sliding force of block n and block $n-1$; Ψ_n is the transfer coefficient; F_s is the stability factor; G_n is the weight of the block n; φ_n is the internal friction angle of the block n along the sliding surface; c_n is the cohesion of the block n along the sliding surface; β_n, β_{n-1} are the slope angle of the block n, block $n-1$ at the bottom, respectively; l_n is the length of the block n along the sliding surface.

The force f is composed of two parts. One is the cohesion on the sliding surface, and the other one is the friction on the sliding surface. Then,

$$f = B \times c + Bh_1\rho\tan\varphi \tag{4}$$

In the equation, ρ is the density of the ELB body; h_1 is the height of part I; c is the cohesion of the ELB body, and φ is the internal friction angle of the ELB body; B is the width of the body.

The passive earth pressure E_p can be calculated according to the following equation.

$$E_p = 1/2 \times \gamma h_1^2 \tan^2(45^\circ + \frac{\varphi}{2}) + 2ch_1 \tan(45^\circ + \frac{\varphi}{2}) \tag{5}$$

By substituting Equations (2)–(5) into Formula (1), we obtain Equation (6).

$$F_s = B(c + h_1\rho\tan\varphi)/(G_n \sin\beta_n) + W \tag{6}$$

where

$$W = \tan\beta_n \tan\varphi_n + \left(c_n l_n + \frac{1}{2} \times \gamma h_1^2 \tan^2(45^\circ + \frac{\varphi}{2}) + 2ch_1 \tan(45^\circ + \frac{\varphi}{2}) - F_{n-1}\psi_n\right)/G_n \sin\beta_n$$

For a given subgrade and the site, the physical and mechanical parameters are determined. Then, W is a constant value. In Equation (6), only F_s and B are variables. From Equation (6), it can be seen that the stability factor F_s is positively correlated with the ELB width B. With the increase in the ELB width, the subgrade stability factor F_s increases accordingly.

3.2. The Relationship between the Subgrade Stability Factors and the ELB Height

Assuming that the strength of the ELB is great enough, ELB shear failure does not occur. The overturn failure will occur as shown in Figure 5. E_a is the active earth pressure; F_n is the landslide pushing force; and E'_p is the passive earth pressure. l is the distance from the E'_p application point to the ELB bottom. m is the distance from the F_n application point to the ELB bottom.

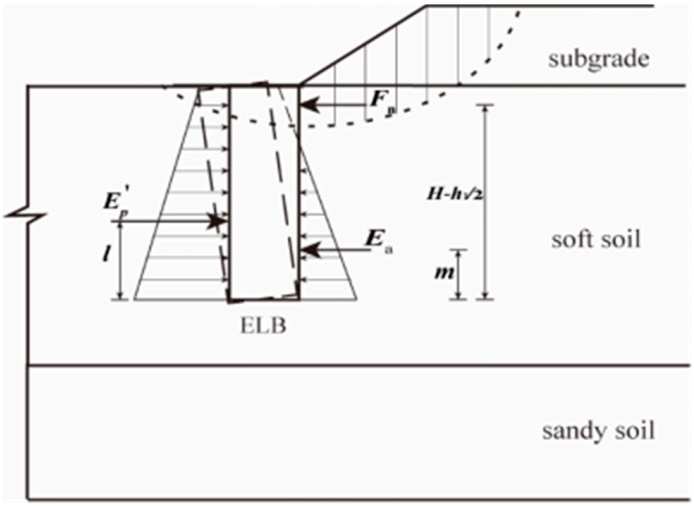

Figure 5. Diagram of the ELB overturn failure.

When the ELB is in a critical state, the torque on the ELB equals zero. Then,

$$M_h = 0 \tag{7}$$

The torque equilibrium equation is established as follows.

$$E'_p \cdot l = F_n \cdot (H - \frac{h_1}{2}) + E_a \cdot m \tag{8}$$

where $l = \frac{H}{3}\frac{\gamma H K_p + 6c\sqrt{K_p}}{\gamma H K_p + 4c\sqrt{K_p}}$, $m = \frac{\gamma H K_a - 2c\sqrt{K_a}}{3\gamma K_a}$.

The passive earth pressure E'_p can be calculated as follows.

$$E'_p = 1/2 \times \gamma H^2 \tan^2(45^\circ + \frac{\varphi}{2}) + 2cH\tan(45^\circ + \frac{\varphi}{2})K_p = \tan^2(45^\circ + \frac{\varphi}{2}) \tag{9}$$

The active earth pressure E_a can be calculated as follows.

$$E_a = 1/2 \times \gamma H^2 \tan^2(45^\circ - \frac{\varphi}{2}) - 2cH\tan(45^\circ - \frac{\varphi}{2}) + \frac{2c^2}{\gamma}K_a = \tan^2(45^\circ - \frac{\varphi}{2}) \tag{10}$$

Substituting Equations (2), (3), (9) and (10) into Equation (8), we obtain Equation (11). Since H is much larger than h_1, H-$h_1/2$ can be replaced by H.

$$F_s = PH^2 + QH + R/H + U - F_{n-1}\psi_n / G_n \sin\beta_n \tag{11}$$

where

$$P = \left(\frac{\gamma K_p}{6} \frac{\gamma H K_p + 6c\sqrt{K_p}}{\gamma H K_p + 4c\sqrt{K_p}} - \frac{\gamma K_a}{6} \right) / G_n \sin \beta_n$$

$$Q = \left(\frac{2c\sqrt{K_p}}{3} \frac{\gamma H K_p + 6c\sqrt{K_p}}{\gamma H K_p + 4c\sqrt{K_p}} + c\sqrt{K_a} \right) / G_n \sin \beta_n$$

$$U = \left(G_n \cos \beta_n \tan \varphi_n + c_n l_n - \frac{2c^2}{\gamma} \right) / G_n \sin \beta_n$$

$$R = \left(\frac{4c^3}{3\gamma^2 \sqrt{K_a}} - \frac{G_n \cos \beta_n \tan \varphi_n h_1}{2} - \frac{c_n l_n h_1}{2} \right) / G_n \sin \beta_n$$

In Equation (11), γ is soil unit weight; K_a is the active earth pressure coefficient; K_p is the passive earth pressure coefficient; F_n and F_{n-1} are the residual sliding force of the block n and block $n-1$, respectively; Ψ_n is the transfer coefficient; F_s is the stability factor; G_n is the weight of the block n; φ_n is the internal friction angle of block n along the sliding surface; c_n is the cohesion of block n along the sliding surface; β_n is the bottom slope angle of block n; l_n is the length of block n along the sliding surface; h_1 is the height of the ELB above the sliding surface.

Equation (11) shows that the stability factor F_s is positively correlated with the square of ELB height H. The stability factor F_s increases with the increase in the ELB height H. In a word, the stability factor F_s increases when the ELB height H and width B increase. The above analytical model can be used to design the subgrade and evaluate the subgrade stability.

There are some assumptions for the above derivation process. For example, the soil pressure on the ELB is simplified as a horizontal force. In addition, from Equations (6) and (11), it is known that there are other parameters influencing the subgrade stability, such as ELM density, cohesion, and internal friction. Therefore, it is necessary to further study the influences of these parameters on the stability factors since experimental tests have high requirements for equipment and costs [23] and it is difficult to explore the influences of these parameters on the stability factors using Equations (6) and (11). However, numerical simulation is an efficient method to further study the influences of these parameters on the ELB stability factors.

4. Numerical Simulation for the Highway Subgrade Stability

4.1. Numerical Model

To verify the theoretical results, a numerical simulation was carried out to study the subgrade stability in this paper. The numerical model was established using Flac^{3D}. As shown in Figure 6, the numerical model consists of four parts. The upper part is the subgrade; the middle part is the soft soil; the lower part is the sandy soil. There are two ELBs at the foot of the subgrade. The width of the subgrade top is 33 m; the height of the subgrade is 6 m; the subgrade slope ratio is 1:1.5; the heights of soft soil and sandy soils are 20 m and 10 m, respectively; the length of soft soil and sandy soil is 91 m. The width of the model is 1 m.

In the model, the hexahedral mesh was used for establishing all layers. Mesh sizes are 1.00 m, 1.00 m, and 1.00 m, respectively, in the X, Y, and Z directions for the soft soil and sandy soil layer. There are 91 mesh elements in the X direction, 1 mesh element in the Y direction, and 30 mesh elements in the Z direction. There are a total of 2730 mesh elements for the soft soil and sandy soil layer. At the subgrade bottom, mesh sizes are also 1 m in the X and Y directions, respectively. At the subgrade top, the total number of mesh elements is 306, which is the same as at the subgrade bottom.

As shown in Figure 6, the X direction displacement is fixed on the left and right boundaries. The Y direction displacement is fixed on the front and back boundaries. The X,

Y, and Z direction displacements are fixed on the bottom boundary. The other boundaries of the model are free. The Mohr–Coulomb constitutive model was adopted for every layer.

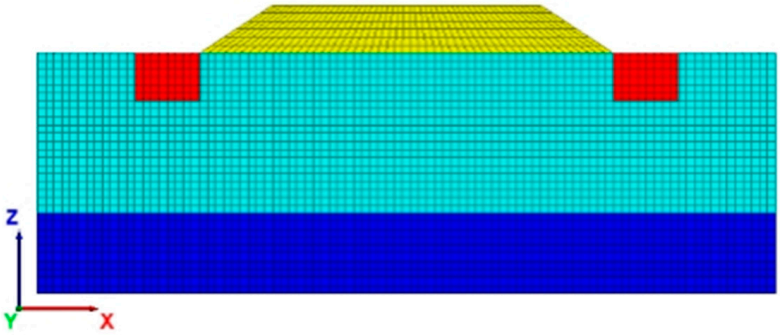

Figure 6. Numerical calculation model of ELB.

The physical and mechanical parameters of the model can be found with a laboratory test. The parameters of the ELB are the same as those of the subgrade. The parameters for all layers are provided in Table 1.

Table 1. Physical and mechanical parameters of the model.

Height/*H*	Unit Weight γ/kN/m^3	Elastic Modulus *E*/MPa	Poisson Ratio v	Cohesion *c*/kPa	Internal Friction Angle φ/°
Subgrade and ELB	19	50	0.3	20	24
Soft soil	17	24	0.35	8	6
Sandy soil	21	60	0.22	390	31.1

4.2. Scheme of Numerical Simulation

To reveal the influences of the ELB on the subgrade stability, a study was carried out on the stability of the subgrade with different ELB widths *B* and heights *H*. The values of the ELB width are 3 m, 4 m, 5 m, and 6 m, respectively. The values of the ELB length are 5 m, 7.5 m, and 10 m, respectively. The subgrade stability factors are calculated by the strength reduction method.

The stability factor of the subgrade without the ELB was calculated first. Then, the stability factors of the subgrade with different ELB widths *B* and heights *H* were calculated. Lastly, an orthogonal test method was carried out to explore ELB parameter sensitivity to the subgrade stability.

4.3. Numerical Results and Discussion

4.3.1. The Stability of the Subgrade without and with ELB

Figure 7 shows the shear strain increment contour of the model without ELB. It can be seen that the sliding surface runs through the subgrade and the soft soil layer. That is to say, the sliding failure occurs in the model. The stability factor of the subgrade is only 1.03. It can be concluded that the subgrade is in a critical state and prone to be unstable if it is not reinforced.

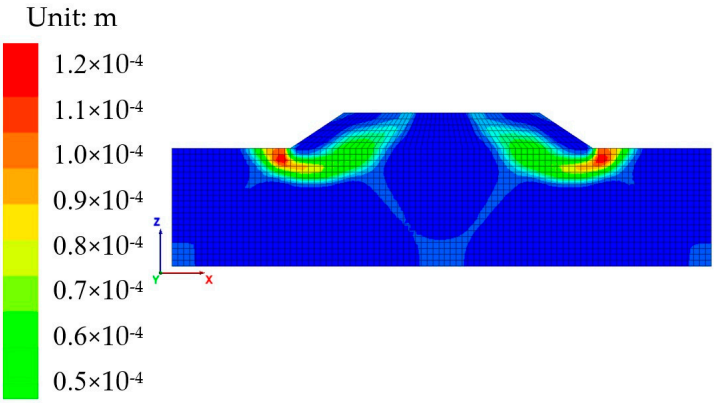

Figure 7. Shear strain increment contour of the model without ELB.

Figure 8 shows the shear strain increment contour of the model with ELB. The height and width of the ELB are 6 m and 10 m, respectively. Figure 8 demonstrates that the sliding surface does not run through the subgrade and the sliding failure does not occur in the subgrade. The stability factor of the subgrade is 1.26. This tells us that the stability of the subgrade can be improved by the ELB.

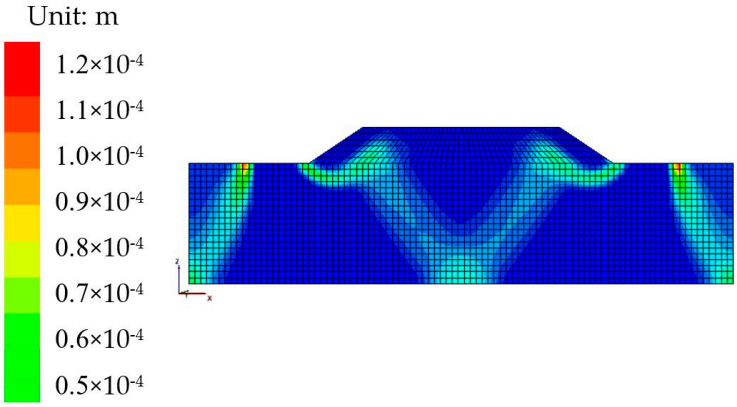

Figure 8. Shear strain increment contour of the model with ELB (H = 6 m, B = 10 m).

4.3.2. Influences of ELB Width on the Subgrade Stability

According to the Chinese Technical Code of Building Slope Engineering (GB50330-2013), the safety factor of the subgrade is 1.25. Figure 9 shows the relationship between the stability factors and the ELB width. It can be seen that the stability factors of the subgrade increase with the increase in ELB width. This is agreeable with the analysis results in Section 3.1. It is found that the stability factors of the subgrade with the ELB are greater than those of the subgrade without the ELB (F_S = 1.03). The stability factors of the subgrade with width B = 10 m and height H = 6 m increase by 22.33% compared with those of the subgrade without the ELB.

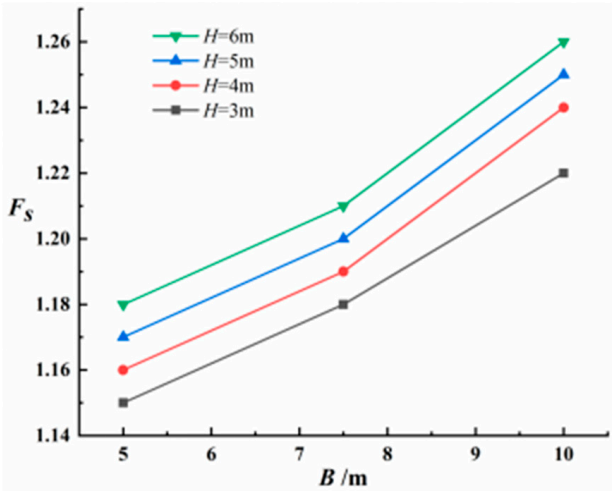

Figure 9. The stability factors of the subgrade with different ELB widths.

A linear equation was utilized to fit the relationship between the stability factors and the ELB width. The fitting formula and correlation coefficient are shown in Table 2. When ELB height H = 3 m, the slope of the fitting formula is 0.014. When ELB height H = 4 m, 5 m, and 6 m, the slopes of the fitting formula are all 0.016. The correlation coefficients are higher than or equal to 0.98 for every fitting formula. The correlation coefficient is very high. It suggests that the stability factors of the subgrade increase linearly with the ELB width increase. This relationship is consistent with the analytical results in Section 3.1.

Table 2. Fitting formula between the stability factor and ELB width.

Height/H	Fitting Formula	Correlation Coefficient
3 m	$F_s = 0.014B + 1.08$	0.99
4 m	$F_s = 0.016B + 1.08$	0.98
5 m	$F_s = 0.016B + 1.08$	0.98
6 m	$F_s = 0.016B + 1.10$	0.98

4.3.3. Influences of ELB Height on the Subgrade Stability

Figure 10 shows the relationship between the stability factors and the ELB height (B = 5 m, B = 7.5 m, B = 10 m). The stability factors increase gradually with the ELB height increase. This is also agreeable with the analytical results in Section 3.2. The relationship between the stability factors and the ELB height was fitted using a linear equation. The fitting formula and correlation coefficients are shown in Table 3. The correlation coefficients are equal to or more than 0.97. This implies that the linear equation is good for fitting the relationship. From Table 3, it is seen that the slope of the fitting formula is 0.01 for the ELB width B = 5 m and B = 7.5 m. The slope is 0.013 for the ELB width B = 10 m. The slopes of the fitting formula increase with the ELB width increase.

Table 3. Fitting formula between the stability factor and ELB height.

Width/B	Fitting Formula	Correlation Coefficient
5 m	$F_s = 0.01H + 1.08$	1.00
7.5 m	$F_s = 0.01H + 1.08$	1.00
10 m	$F_s = 0.013H + 1.08$	0.97

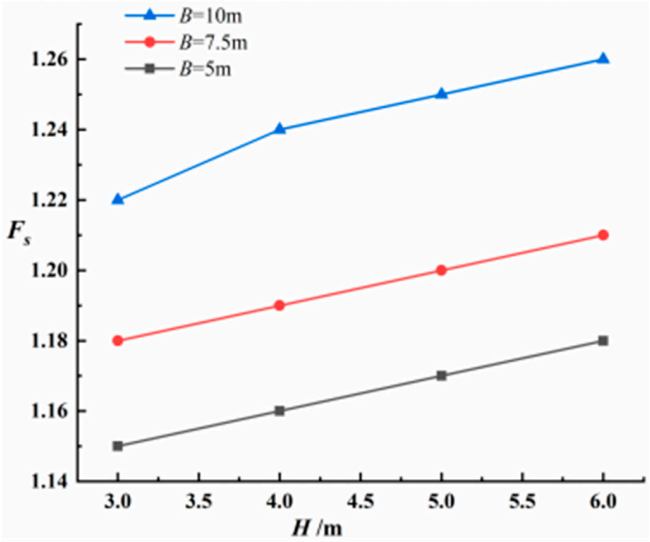

Figure 10. The stability factors of the subgrade with different ELB heights.

In Table 2, the minimum slope of the fitting formula is 0.014, while the maximum slope of the fitting formula in Table 3 is 0.013. The slope of the fitting formula in Table 2 is greater than that in Table 3. This means that the increased ratio of stability factors with the width increase is greater than that with the height increase. It can be concluded that the influences of ELB width on the subgrade stability factor are greater than that of ELB height. This is consistent with Chen's research conclusion [8].

In summary, with the ELB width and height increase, the subgrade stability factors increase. The ELB width has a greater influence on the subgrade stability factors than the ELB height. For the ELB design, the scheme with bigger ELB width is recommended to ensure subgrade stability.

5. Parameter Sensitivity Analysis

As mentioned above, there are multiple ELB parameters influencing the subgrade stability. To explore the relative influences of every parameter on the subgrade stability, the sensitivity analysis of ELB parameters is necessary to be carried out. The sensitivity analysis can be conducted by the parameter tuning method, the alternating method, the parallel line method, and the bisection method. However, these methods are not suitable for the multiple factor sensitivity analysis. So, for the ELB parameters' sensitivity to the subgrade stability, the multiple factor methods should be used.

The orthogonal test method is a multiple-factor sensitivity analysis method. In this paper, it is used to explore the ELB parameters' sensitivity to subgrade stability. This method combines numerical simulation with probability and statistics theory, which can reduce the test number.

5.1. Parameter Selection

The width and height are all geometric parameters. As can be seen from the above analysis in Section 4.3, the ELB width and height have a great influence on the subgrade stability. Therefore, these geometric parameters' sensitivity should be explored. If the ELB strength is not enough, subgrade plastic deformation and failure will occur. Therefore, the sensitivity of the physical and mechanical parameters should also be explored. In a word, the parameters selected for the sensitivity analysis are width, height, density, cohesion, and internal friction angle. The values of every parameter were determined from the value of compacted soil parameters in the literature. In this paper, the values are divided into five levels for every parameter. The parameter values for every level are shown in Table 4.

Table 4. ELB parameter values for every level.

Level	Parameters				
	Width *B*/m	**Height *H*/m**	**Density ρ/kg/m^3**	**Cohesion *c*/kPa**	**Internal Friction φ/°**
level 1	2.5	2	1700	10	8
level 2	5	3	1800	12.5	12
level 3	7.5	4	1900	15	16
level 4	10	5	2000	17.5	20
level 5	12.5	6	2100	20	24

5.2. Sensitivity Analysis

The five-factor and five-level orthogonal test was selected. There are twenty-five cases for the orthogonal test. The stability factors were calculated using the FLAC^{3D} software for every case. The orthogonal test scheme and stability factors are shown in Table 5.

Table 5. Orthogonal test scheme and stability factors.

No.	Factors					F_s
	Factor A	**Factor B**	**Factor C**	**Factor D**	**Factor E**	
	Width *B*/m	**Height *H*/m**	**Density ρ/kg/m^3**	**Cohesion *c*/kPa**	**Internal Friction φ/°**	
1	2.5	2	1700	10	8	1.11
2	5	2	1800	12.5	12	1.13
3	7.5	2	1900	15	16	1.16
4	10	2	2000	17.5	20	1.18
5	12.5	2	2100	20	24	1.22
6	2.5	3	2000	12.5	16	1.14
7	5	3	2100	15	20	1.16
8	7.5	3	1700	17.5	24	1.16
9	10	3	1800	20	8	1.17
10	12.5	3	1900	10	12	1.18
11	2.5	4	1800	15	24	1.14
12	5	4	1900	17.5	8	1.16
13	7.5	4	2000	20	12	1.20
14	10	4	2100	10	16	1.21
15	12.5	4	1700	12.5	20	1.18
16	2.5	5	2100	17.5	12	1.16
17	5	5	1700	20	16	1.16
18	7.5	5	1800	10	20	1.18
19	10	5	1900	12.5	24	1.21
20	12.5	5	2000	15	8	1.24
21	2.5	6	1900	20	20	1.16
22	5	6	2000	10	24	1.17
23	7.5	6	2100	12.5	8	1.19
24	10	6	1700	15	12	1.18
25	12.5	6	1800	17.5	16	1.23

K_{ij} is the sum of all test results for each factor at the same level. R_j is the range of the factor j. It can be calculated as followed

$$R_j = \max\{K_{1j}, K_{2j}, K_{3j}, K_{4j}, K_{5j}\} - \min\{K_{1j}, K_{2j}, K_{3j}, K_{4j}, K_{5j}\}.$$

The range R_j is a variable. If the R_j value is larger, the influences of factor j on the subgrade stability are greater. Therefore, a larger range R_j value indicates that the subgrade stability is more sensitive to the factor j. The range R_j can be used to determine the sensitivity order of every factor. The range analysis results are shown in Table 6.

Table 6. Range analysis results.

	Width *B*/m	Height *H*/m	Density ρ/kg/m^3	Cohesion *c*/kPa	Internal Friction φ/°
K_{1j}	5.71	5.8	5.80	5.85	5.87
K_{2j}	5.78	5.81	5.85	5.85	5.85
K_{3j}	5.89	5.89	5.87	5.88	5.9
K_{4j}	5.95	5.95	5.93	5.89	5.86
K_{5j}	6.05	5.93	5.94	5.91	5.9
R_j	0.34	0.15	0.14	0.06	0.05

Table 6 and Figure 11 demonstrate that R_A is the biggest, R_B, R_C, and R_D are next, and R_E is the smallest. These suggest that the ELB width is the most sensitive parameter and the internal friction is the least sensitive parameter. The ELB width's sensitivity to the stability factors is higher than that of ELB height. This is consistent with the simulation results in Section 4.

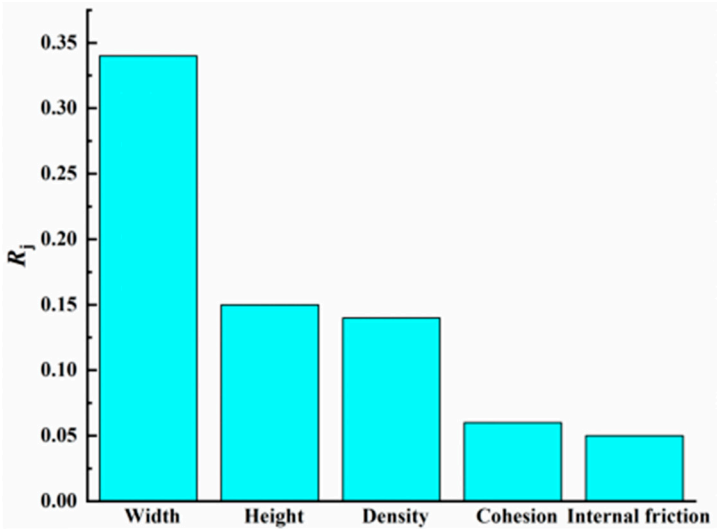

Figure 11. The range for every factor.

The R_B is higher than R_C. This means the sensitivity of the geometric parameters (width, height) is higher than that of the physical and mechanical parameters. The R_C is higher than R_D, which shows the ELB density's sensitivity to the stability factors is higher than that of ELB cohesion. The ELB parameter sensitivity order is as follows. Width > height > density > cohesion > internal friction.

In the ELB designing process, the width and height should be focused on and the density, cohesion, and internal friction can be ignored.

6. Conclusions

In this paper, the stability of the subgrade with ELB is described using theoretical and numerical simulation methods. The following conclusions are drawn.

(1) An analytical model was proposed for stability analysis of the subgrade with ELB, and it can be used for ELB design.

(2) The subgrade stability can be improved drastically by the ELB. With the ELB width and height increase, the subgrade stability factors increase gradually. The subgrade stability factors increase more with the width increase than that with the height increase. That is, the ELB width has a greater influence on the subgrade stability factors than the ELB height. For the ELB design, the ELB with bigger width is recommended to ensure subgrade stability.

(3) The ELB parameter sensitivity order on the subgrade stability is as follows. Width > height > density > cohesion > internal friction. In the ELB designing process, the width and height should be focused on and the density, cohesion, and internal friction can be ignored.

This research provides references for ELB designing and is significant for promoting the application of ELB in soft soil areas. In future, research on the ELB designing method can be carried out.

Author Contributions: Conceptualization, F.X.; methodology, F.X., X.W., F.Y. and J.Y.; software, L.H.; validation, R.L. and J.Y.; investigation, X.W. and F.Y.; resources, X.W.; writing—original draft preparation, F.X.; writing—review and editing, X.W. and F.Y.; visualization, L.H. and X.W.; supervision, R.L.; project administration, R.L.; funding acquisition, F.X. All authors have read and agreed to the published version of the manuscript.

Funding: This research was funded by the Natural Science Foundation of Anhui Province (Grant No. 2108085ME190).

Institutional Review Board Statement: Not applicable.

Informed Consent Statement: Not applicable.

Data Availability Statement: The raw data required to reproduce these findings cannot be shared at this time due to time limitations. The processed data required to reproduce these findings cannot be shared at this time due to time limitations.

Acknowledgments: The authors would like to acknowledge the China Railway No. 4 Engineering Group Co., Ltd.

Conflicts of Interest: The authors declare no conflict of interest.

References

1. Shan, Y.; Wang, X.; Cui, J.; Mo, H.H.; Li, Y.D. Effects of clay composition on the dynamic properties and fabric of artificial marine clay. *J. Mar. Sci. Eng.* **2021**, *9*, 1216. [CrossRef]
2. Shen, J.H.; Hu, M.J.; Wang, X.; Zhang, C.Y.; Xu, D.S. SWCC of calcareous silty sand under different fines contents and dry densities. *Front. Environ. Sci.* **2021**, *9*, 1–13. [CrossRef]
3. Zhu, M. Selection of reasonable cross-section of embankment in soft soil region. *China Civ. Eng. J.* **1964**, *11*, 48–60. (In Chinese)
4. Zhang, X.; Li, X.; Shen, Y.P. Study on foundation treatment scheme of high embankment in soft soil section of Mombasa West Railway Station. *Subgrade Eng.* **2018**, *03*, 229–233.
5. Corkum, A.G.; Martin, C.D. Analysis of a rock slide stabilized with a toe-berm: A case study in British Columbia, Canada. *Int. J. Rock Mech. Min. Sci.* **2004**, *7*, 1109–1121. [CrossRef]
6. Zaytsev, A.; Petriaev, A.; Erniauskaite, L. Track structure reconstruction practice for the subgrade on weak foundation soil. In Proceedings of the Fifth International Conference on Road and Rail Infrastructure, Zadar, Croatia, 17–19 May 2018.
7. Viswanadham, B.V.S.; Das, A.V.; Mathur, K. Centrifuge Model Tests on Rail Embankments Constructed with Coal Ash as a Structural Fill Material. In Proceedings of the GeoCongress 2012: State of the Art and Practice in Geotechnical Engineering, San Francisco, CA, USA, 25–29 March 2012.
8. Chen, J.F.; Song, E. Optimized design of loading berm for Highfill slope of the airport in the mountainous area of southwest China. *Eng. Mech.* **2012**, *29*, 85–97.
9. Zhao, N.Y.; Liang, B.; Huang, F.; Liu, Y. An analytical design method for loading berm of fill embankment. *Rock Soil Mech.* **2015**, *36*, 2914–2920.
10. Isamu, M. Some aspects of road construction over peat or marshy areas in Hokkaido with particular reference to filling method. *Soils Found.* **1960**, *33*, 99–107.
11. Ishola, V.L.C.; Yan, M.H.; Ling, X.Z.; Tang, L.; Ogoubi, C.A. Dynamic Response Analysis Of Geogrid Reinforced Embankment Supported by CFG Pile Structure During A High-Speed Train Operation. *Lat. Am. J. Solids Struct.* **2019**, *16*, 1–20.
12. Gao, J.L.; Xie, X.L.; Wang, J.J.; Liu, L.; Zhang, W.J. Numerical And Theoretical Analysis Of Geosynthetic Encased Stone Column Composite Foundation Under Cyclic Loading. *Lat. Am. J. Solids Struct.* **2022**, *19*, 1–15. [CrossRef]
13. Roy, D.; Singh, R. Mechanically stabilized earth wall failure at two soft and sensitive soil sites. *J. Perform. Constr. Facil.* **2008**, *22*, 373–380. [CrossRef]
14. Griffths, D.V.; Lane, P.A. Slope stability analysis by finite elements. *Geotechnique* **1999**, *49*, 387–403. [CrossRef]
15. Austin, S.; Jerath, S. Mahdi, Effect of soil-foundation-structure interaction on the seismic response of wind turbines. *Ain Shams Eng. J.* **2017**, *8*, 323–331. [CrossRef]

16. Alreja, J.; Parab, S.; Mathur, S.; Samui, P. Estimating hysteretic energy demand in steel moment resisting frames using Multivariate Adaptive Regression Spline and Least Square Support Vector Machine. *Ain Shams Eng. J.* **2016**, *6*, 449–455. [CrossRef]
17. Zienkiewicz, O.C.; Humpheson, C.; Lewis, R.W. Associated and non-associated visco-plasticity and plasticity in soil mechanics. *Geotechnique* **1975**, *25*, 671–689. [CrossRef]
18. Ma, Y.C.; Su, P.D.; Li, Y.G. Three-dimensional nonhomogeneous slope failure analysis by the strength reduction method and the local strength reduction method. *Arab. J. Geosci.* **2020**, *13*, 21. [CrossRef]
19. Zhang, Y.C.; Yang, G.H.; Hu, H.Y.; Zhang, Y.X. Stability study of embankment or dam with back berm on soft soil foundation. *Rock Soil Mech.* **2007**, *28*, 844–848.
20. Robert, M.E.; John, F.P.; Reed, L.M. The roles of non-linear deformation analyses in the design of a reinforced soil berm at Red River U-frame lock No. 1. *Int. J. Numer. Anal. Methods Geomech.* **1997**, *21*, 753–787.
21. Khosravifardshirazi, A.; Johari, A.; Javadi, A.A.; Khanjanpour, M.H.; Khosravifardshirazi, B.; Akrami, M. Role of Subgrade Reaction Modulus in Soil-Foundation-Structure Interaction in Concrete Buildings. *Buildings* **2022**, *12*, 540. [CrossRef]
22. Daweon, E.M.; Roth, W.H.; Drescher, A. Slope stability analysis by strength reduction. *Geotechnique* **1999**, *49*, 835–840.
23. Qin, G.; Yang, F.; Jin, D.Q. Stress Transferring Mechanism of a Pressure Tunnel Lining Strengthened with CFRP. *Lat. Am. J. Solids Struct.* **2021**, *18*, 1–18. [CrossRef]